Neural Comput & Applic (2019) 31:3227–3243
DOI 10.1007/s00521-017-3264-5

ORIGINAL ARTICLE

A stochastic well-test analysis on transient pressure data using iterative ensemble Kalman filter

Hamid Bazargan[1] · **Meisam Adibifard**[2]

Received: 8 April 2017 / Accepted: 15 October 2017 / Published online: 4 November 2017

Abstract Accurate estimation of the reservoir parameters is crucial to predict the future reservoir behavior. Well testing is a dynamic method used to estimate the petrophysical reservoir parameters through imposing a rate disturbance at the wellhead and recording the pressure data in the wellbore. However, an accurate estimation of the reservoir parameters from well-test data is vulnerable to the noise at the recorded data, the non-uniqueness of the obtained match, and the accuracy of the optimization algorithm. Different stochastic optimization methods have been applied to this address problem in the literature. In this study, we apply the recently developed iterative ensemble Kalman filter in the context of well-test analysis to infer reservoir parameters from the noisy recorded data. Since the introduction of the ensemble Kalman filter (EnKF) by Evensen in 1994 as a novel method for data assimilation, it has had enormous impact in many application domains because of its robustness and ease of implementation, and numerical evidence of its accuracy. While the objective of the standard EnKF approaches is to approximate the statistical properties of geological parameters conditioned to observation, via an ensemble, the objective of the iterative ensemble Kalman methods is to approximate the solution of inverse problems using a deterministic derivative-free iterative scheme. We conducted three case studies of the application of the iterative ensemble Kalman methods for a well-test analysis of a homogenous reservoir model, a dual-porosity heterogeneous system, and a faulted discontinuous reservoir. We demonstrated that the convergence occurs very rapidly almost at the first iterations contrary to the well-known particle swarm optimization algorithm. The maximum relative error for the simulated cases is below 15%, which belongs to the skin factor. Low relative error, narrowed uncertainty range over time, and excellent graphical match obtained between the simulated derivative data and the generated curve by using the iterative EnKF verify the robustness of the developed algorithm even in dealing with complex heterogeneous models.

Keywords Pressure transient · Data assimilation · Iterative ensemble Kalman filter · Stehfest algorithm

Nomenclatures

$u_{(k+1)}$	State parameters of the system at the $k+1$th iteration within the Kalman filter
u_k	State parameters of the system at the kth iteration within the Kalman filter
A_k	A matrix relating state parameters at the kth iteration to the $k+1$th iteration within the Kalman filter
B	A matrix relating the inputs at the kth iteration to the $k+1$th iteration
x_k	System's input data
h_k	System noise at the kth iteration
v_k	Measurements noise at the kth iteration
y_k	Observational data at the kth iteration
H_k	A matrix relating the state parameters at the kth iteration to the observations at the kth iteration
$F(\psi)$	Probability density of the model states

Hamid Bazargan and Meisam Adibifard have equally contributed to this work.

✉ Meisam Adibifard
ma1808@msstate.edu

[1] Energy Engineering Department, Sharif University of Technology, Tehran, Iran

[2] Dave C. Swalm School of Chemical Engineering, Mississippi State University, Starkville, MS, USA

f_i	Component number i of the model operator f
gQg^T	Covariance matrix for the model errors
Q	Variance of the systems' noise
R	Variance of the measurement's noise
$P(h)$	Probability function governing the system's noise
$P(v)$	Probability function describing the measurements' noise
T	Time, hr
J	Number of ensembles within the EnKF algorithm
$y^{(j)}$	Measurements for the jth ensemble in the EnKF algorithm
$\xi^{(j)}$	Measurements' noise for the jth ensemble within the EnKF
Γ	Variance of the measurements' noise
$w_n^{(j,f)}$	Predicted state parameters in the EnKF method for the jth ensemble within the EnKF method
G	Nonlinear model operator
$u_n^{(j)}$	State parameters at the nth iteration for the jth ensemble in the EnKF method
$\bar{w}_n^f$	Ensemble average of the predicted state parameters in the nth iteration within the EnKF method
$\bar{u}_n$	Ensemble average of the state parameters in the nth iteration within the EnKF method
C_n^{uw}	The cross-covariance matrix of the state parameters and the estimated state parameters at the iteration n
C_n^{ww}	The autocorrelation matrix of the estimated state parameters at the iteration n
$u_{(n+1)}^{(j)}$	Estimated state parameters belonging to the jth ensemble at the $n+1$th iteration after applying the analysis step in the EnKF method
$w_{(n+1)}^{(j)}$	Predicted state parameters belonging to the jth ensemble at the $n+1$th iteration within the EnKF method
$\bar{u}_{(n+1)}$	Ensemble average of the state parameters at the $n+1$th iteration
t_{D}	Dimensionless time
p_{wd}	Well dimensionless pressure
s	Laplace variable
$\bar{p}_{\mathrm{wd}}(s)$	Well dimensionless pressure solution in the Laplace domain
Φ	Porosity fraction
r_w	Wellbore radius, ft
h	Reservoir thickness, ft
c_t	Total compressibility, psi^{-1}
q	Well flow rate, STBD
p_i	Initial pressure, psi
μ	Viscosity, cp
B_o	Oil Formation Volume Factor, Rbbl/STB
K	Permeability, md
S	Skin factor, dimensionless
Λ	Interporosity flow coefficient, dimensionless
ω	Fracture storativity ratio, dimensionless
L_f	Perpendicular fault distance from well, ft
$f(s)$	Laplace function for the dual-porosity model
k_0	Modified Bessel function of second kind and zero degree
k_1	Modified Bessel function of second kind and first degree
C_{D}	Dimensionless wellbore storage coefficient, dimensionless
d_{D}	Fault dimensionless distance, dimensionless

1 Introduction

Modern calibration methods of subsurface reservoirs can be generally classified into two approaches, one based on the optimization methods and the other based on the Bayesian inference [1]. The optimization methods adjust the unknown parameter values through an automated process to obtain reservoir models within the allowed range of a misfit function. Various optimization techniques have been developed in the literature, including neighborhood algorithm [2], particle swarm optimization [3], genetics algorithm [4], Levenberg–Marquardt [5], estimation of distribution [6], and LBFGS [7]. Existing optimization methods can be roughly categorized to the stochastic algorithms and the gradient-based algorithms. The gradient-based algorithms have several inherent limitations, including they require to compute the gradients at each step of the optimization process. Honoring the geological constraint is another challenging issue for these types of algorithms [8]. A definite advantage of the stochastic algorithms is the capability to easily honoring the geological constraints; the main drawback of these approaches is their inefficiency as they usually require large number of simulations for convergence [9, 10]. Approaches based on the Bayesian inference, on the other hand, aim at estimating the posterior probability for the reservoir properties [11]. Existing Bayesian inference methods broadly entail algorithms based on particle filters, such as the ensemble Kalman filter (EnKF) [12, 13], the sequential Monte Carlo methods [14], and the Markov Chains Monte Carlo (MCMC) approaches [15, 16]. Since characterization of the underground resources becomes very important especially during the tertiary recovery period, which most of the oil is still remained beneath the ground [17], opting a robust and efficient method during the reservoir's calibration is of great importance.

Although variety of data mining, artificial intelligence, and optimization algorithms are used in the petroleum industry for different purposes [18–30], in the context of well-test analysis most researches are carried out over the application of the artificial neural networks (ANN), nonlinear regression, and meta-heuristic optimization algorithms.

The first attempt to incorporate ANN in the well-testing interpretation comes back to 1990s when Al-Kaabi et al. [31] used normalized pressure-derivative data in log–log plot to train an ANN with the purpose of reservoir model recognition. Allain and Houze [32] tried to symbolically represent a reservoir model using the ANN method. Within the next year, Ershaghi et al. [33] employed multiple neural nets to recognize patterns for a specific conceptual reservoir model. They found that an activation number larger than 0.4 for a neuron is usually sufficient to select the reservoir model related to that neuron [33].

Athichanagorn and Horne [34] employed ANN in order to recognize eight different mostly appeared pressure patterns in pressure-derivative curves. Kumoluyi et al. [35] used higher-order neural networks to recognize the reservoir model from well-test data. Using higher-order neural networks allowed them to elude large amounts of weights at the neural network, which in turn leads to decreased training time [35]. Alajmi and Ertekin [36] fitted a degree-four polynomial over pressure data in semilog plot and used coefficients of the interpolated polynomial as part of the input data to the ANN. Kharrat and Razavi [37] fitted B-splines curve over pressure data and used its analytical derivative against time to generate pressure-derivative curves. The normalized pressure-derivative data were then given to the ANN in their study [37]. Adibifard et al. [38] introduced a new method to present the input test data to the ANN by fitting a Chebyshev-based polynomial over the synthesized pressure-derivative data. Their proposed method guaranteed fitting higher degrees of polynomials without losing precision over the polynomial coefficients [38].

Although there have been numerous studies, recently, to characterize hydrocarbon reservoirs by introducing different interpretation methods and models[39], accuracy of the estimated parameters is usually a direct function of the optimization technique embedded in the nonlinear regression problem. In this regard, there have been several studies on the applications of nonlinear regression in well-test analysis by using different sets of cost functions including LS (least square), LAV (least absolute value), and weighted cost function [40–42]. Nanba and Horne [43] used a new MGC (modified Gauss–Cholesky) algorithm and justified the superiority of their algorithm over the GM (Gauss–Marquardt) and NB (Newton–Barua). Onur and Kuchuk [44] employed the maximum likelihood approach to carry out the nonlinear regression task. This method does not require acquiring a prior knowledge about the variance of the error data [44]. Recently, Adibifard et al. [45] employed a meta-heuristic optimization algorithm, namely PSO (particle swarm optimization) to carry out the nonlinear regression task for a homogenous reservoir model. A comprehensive review of recent research activities on subsurface flow model calibration can be found in [8, 46].

In this work, we study the application of the iterative ensemble Kalman methods as a derivative-free type of optimization algorithm for inverse problems arises in well-test analysis. Ensemble Kalman-based methods use the Kalman formula to generate an ensemble of posterior estimates of the reservoir parameters [47]. Since its introduction by Evensen in 1994, the number of publications about EnKF has become extensive and has been applied in various research fields entailing oceanography [48–50], numerical weather prediction [51, 52], hydrology [53–55], and petroleum reservoir history matching [13, 56, 57]. A chronological list of applications of EnKF can be found at [12]. Multiple variants of EnKF for state and parameter estimation in dynamic systems can be found at [12, 13, 58]. In essence, all the variants of EnKF use an ensemble of states and parameters that is sequentially updated by means of the Kalman formula, which assimilated the available data at a given time into the model. In this work, we are interested in studying the application of the iterative ensemble Kalman methods [59] for the solution of inverse problems arise in subsurface flow. While the objective of the standard EnKF approaches is to approximate the statistical properties of geological parameters conditioned to observation, via an ensemble, the objective of the iterative ensemble Kalman methods is to approximate the solution of inverse problems 1 using a deterministic derivative-free iterative scheme. Variants of the iterative ensemble methods have been proposed in the literature. Iglesias et al. [59] studied the properties of the iterative EnKF algorithm for inversion and demonstrated numerically that the method can be effective on a wide range of applications. He studied the convergence properties of the iterative regularized ensemble Kalman method and its efficiency comparing to other ensemble-based methods.

The organization of this paper is as follows: Section 2 presents the formulation of the iterative ensemble Kalman method. Section 3 studies the results of the iterative ensemble method for three different cases of well-test analysis, a homogenous reservoir model, a dual-porosity heterogeneous system, and a faulted discontinuous reservoir. Section 4 presents the conclusion and recommendation for future research works.

2 Iterative ensemble Kalman filter (EnKF)

The Kalman filter was developed by Kalman in 1960 in order to estimate the current state of a system by knowing its prior state and the current measurements [60]. This filtering approach is used for the following discrete-time controlled process, which is governed by the linear stochastic difference equation [61]:

$$u_{k+1} = A_k u_k + B x_k + h_k, \tag{1}$$

The above equation relates the state parameters at the kth iteration, i.e., u_k, to the state of the system at the $k+1$th iteration, i.e., u_{k+1}. x_k is also the input of the system, and A and B are corresponding matrices, which make a connection between input, state at the previous time and the state at the next time. The observation data y_k are calculated using the following equation:

$$y_k = H_k u_k + v_k, \tag{2}$$

The random variables h_k and v_k are, respectively, the system and measurement noise, which are considered independent with normal PDF (probability distribution function). The normal PDF has the zero mean and variances of Q and R, respectively, for h and v [61]:

$$P(h) \sim N(0, Q)$$
$$P(v) \sim N(0, R), \tag{3}$$

Although EKF (extended Kalman filter) improves applicability of the Kalman filter for the nonlinear systems through incorporating the Jacobian of the dynamic matrix, it fails to address the entirely nonlinear dynamics [62]; therefore, another variant of Kalman filter is introduced, which is based on the evolution of the ensembles of the state parameters.

The ensemble Kalman filter (EnKF), which is a sequential data assimilation approach, was developed by Evensen [63]. The EnKF method was developed based on the prediction of the error statistics by using the Monte Carlo method and eliminated the unlimited error growth generated during the extended Kalman filter analysis [63]. In the EnKF, the true model is not known and the mean of the parameters is considered as the best estimate; thereby, the spreading of the other ensembles around the mean of the parameters is deemed as the error definition [64].

The EnKF acts as a suboptimal estimator in which the error statistics are forecasted by using the Monte Carlo simulations or ensemble integration in order to solve the following Fokker–Planck equation [62, 64]:

$$\frac{\partial F}{\partial t} + \sum_i \frac{\partial (f_i F)}{\partial u_i} = \frac{1}{2} \sum_{i,j} \frac{\partial F (g Q g^T)_{ij}}{\partial u_i \partial u_j}, \tag{4}$$

where at the above equation, u is the state parameters, $F(u)$ is the probability density of the model states, f_i is the component number i of the model operator f, and $ygQg^T$ is the covariance matrix for the model errors.

The Fokker–Planck equation is the fundamental equation to find the evolution of the error statistics over time. Actually, the EnKF method employs the Monte Carlo simulations to solve the Fokker–Planck equation, and the PDF of the state parameters is represented by using large ensemble models [64]. The merits of EnKF over EKF, in addition to its capability to handle the largely nonlinear systems, are its low computational time for cases with small ensemble size and large iterations [62]. One of the other advantages of the EnKF is that it does not require derivations of the tangent linear operator or the adjoint equations [65]. The iterative EnKF, which is adopted at this study to tackle the pressure transient nonlinear regression problem, is described at the following [59]:

Generate the initial ensembles of state parameters as $\{u_0^j\}_{j=1}^J$, where J is the number of ensembles. Also, regenerate observational data for each ensemble by perturbing the actual measurement data by using the following equation:

$$y^{(j)} = y + \xi^{(j)}, \tag{5}$$

where $\xi^{(j)}$ is picked up from the Gaussian distribution with mean zero, i.e., $\xi^{(j)} \sim N(0, \Gamma)$.

1. Update the state parameters for $n = 1$ to maximum iteration by using the following prediction and analysis steps:

Prediction step:

$$w_n^{(j,f)} = G\left(u_n^{(j)}\right), \quad j \epsilon \{1, \ldots, J\}, \tag{6}$$

where G is the nonlinear operator which maps the unknown state parameters u to the measurement space.

$$\bar{w}_n^f = \frac{1}{J-1} \sum_{j=1}^{J} w_n^{(j,f)}, \tag{7}$$

$$\bar{u}_n = \frac{1}{J-1} \sum_{j=1}^{J} u_n^{(j)}, \tag{8}$$

$$C_n^{uw} = \frac{1}{J-1} \sum_{j=1}^{J} \left(u_n^{(j)} - \bar{u}_n\right)\left(w_n^{(j,f)} - \bar{w}_n^f\right)^T, \tag{9}$$

$$C_n^{ww} = \frac{1}{J-1} \sum_{j=1}^{J} \left(w_n^{(j,f)} - \bar{w}_n^f\right)\left(w_n^{(j,f)} - \bar{w}_n^f\right)^T, \tag{10}$$

Analysis step:

$$u_{n+1}^{(j)} = u_n^{(j)} + C_n^{uw}\left(C_n^{ww} + \Gamma\right)^{-1}\left(y^{(j)} - w_n^{(j,f)}\right), \tag{11}$$

$$w_{n+1}^{(j)} = w_n^{(j)} + C_n^{ww}\left(C_n^{ww} + \Gamma\right)^{-1}\left(y^{(j)} - w_n^{(j,f)}\right), \tag{12}$$

$$\bar{u}_{n+1} = \frac{1}{J-1} \sum_{j=1}^{J} u_{n+1}^{(j)}, \tag{13}$$

Check for convergence at each iteration.

At this paper, the nonlinear G operator is a mathematical model describing the wellbore pressure behavior by using

the unknown well and reservoir parameters, known fluid and rock properties, and the well rate history data. Because of the complexity of the final solution, usually a Laplace inverse algorithm is used to convert the obtained wellbore solution from the Laplace media into the time domain. The Laplace solutions for various reservoir models are provided at Appendix A in the end of the paper. Stehfest algorithm and the method of Okoye et al. [66, 67] are employed at this study to regenerate the pressure derivative versus time data:

$$\left(t_{\mathrm{D}}\frac{\mathrm{d}p_{\mathrm{wd}}}{\mathrm{d}t_{\mathrm{D}}}\right)_i = \left(\frac{\mathrm{d}p_{\mathrm{wd}}}{\mathrm{dln}(t_{\mathrm{D}})}\right)_i = t_{\mathrm{Di}}\left[\mathcal{L}^{-1}\{s\bar{p}_{\mathrm{wd}}(s)\}\right]_{t_{\mathrm{Di}}}. \quad (14)$$

3 Results and discussion

The iterative EnKF is applied to three different case studies entailing a homogenous, a dual-porosity, and a faulted reservoir. We present the well-test analysis using the iterative EnKF for these cases at the following subsections.

3.1 Infinite acting homogenous reservoir

The field data for this experiment belongs to Horne [68]. Due to the stabilization of the pressure-derivative at the end of the wellbore storage region, a homogenous reservoir model is adopted for the matching purpose. Fluid and rock are represented in Table 1. Pressure derivative against time data are provided in the log–log plot in Fig. 1.

The measured derivative data are perturbed with the additive noise of 0.05 × $td p/dt$. Totally, 200 ensembles are used for the EnKF method and the 50th iteration is used as the stopping criteria, as discussed in Igelsias et al. [59]. The convergence study of the iterative EnKF algorithm is not the scope of this study as it has been rigorously addressed in the literature. Six different perturbed versions of the measured data are illustrated in Fig. 2 along with the non-perturbed data.

Figure 3 shows the result of the iterative EnKF algorithm to estimate the PDF (probability distribution function) of the unknown reservoir parameters. Also, the normal function is fitted over the PDF data for each state variable. Figure 4 demonstrates the fast convergence rate

Table 1 Fluid and rock data belonging to the Horne (1995) real case

Φ, fraction	0.21
r_w, ft	0.401
h, ft	23
c_t, psi^{-1}	8.72×10^{-6}
q, STBD	2500
p_i, psi	6009
μ, cp	0.92
B_o, Rbbl/STB	1.21

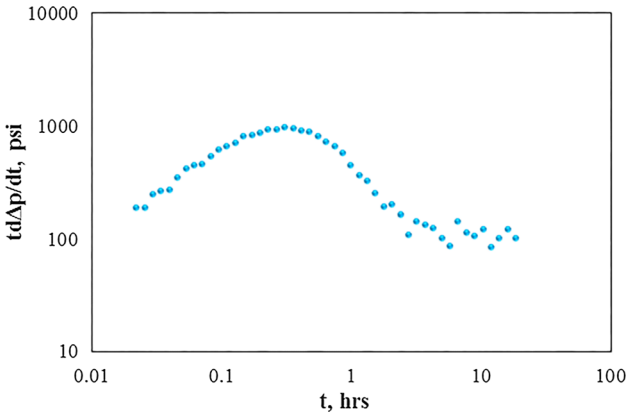

Fig. 1 Logarithmic plot of the pressure derivative versus time or the field case adopted from [68]

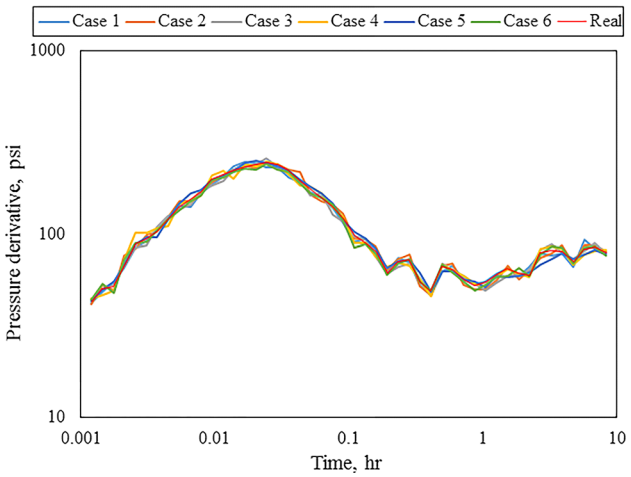

Fig. 2 Various realizations of the derivative data generated for the iterative EnKF method for the data taken from [68]

of the algorithm. Figure 5 shows that the variance of the results tends to decrease rapidly at the initial iterations, which demonstrate the robustness of the iterative EnKF technique to reach the final solution quickly. Table 2 compares the results of the iterative EnKF with those arrived by Adibifard et al. [45] by employing the PSO (particle swarm optimization) algorithm. Obviously, a good agreement is observed between our results and the results belonging to [45].

3.2 Dual-porosity fractured reservoir

For the dual-porosity model, which comprises both matrix and fracture systems, a drawdown test is simulated by using a commercial well-test software and the generated derivative data are used as a reference for data analysis for the iterative EnKF algorithm. Fluid and rock data used for the test simulation are provided in Table 3. In addition, to make the generated data more realistic, a quartz pressure

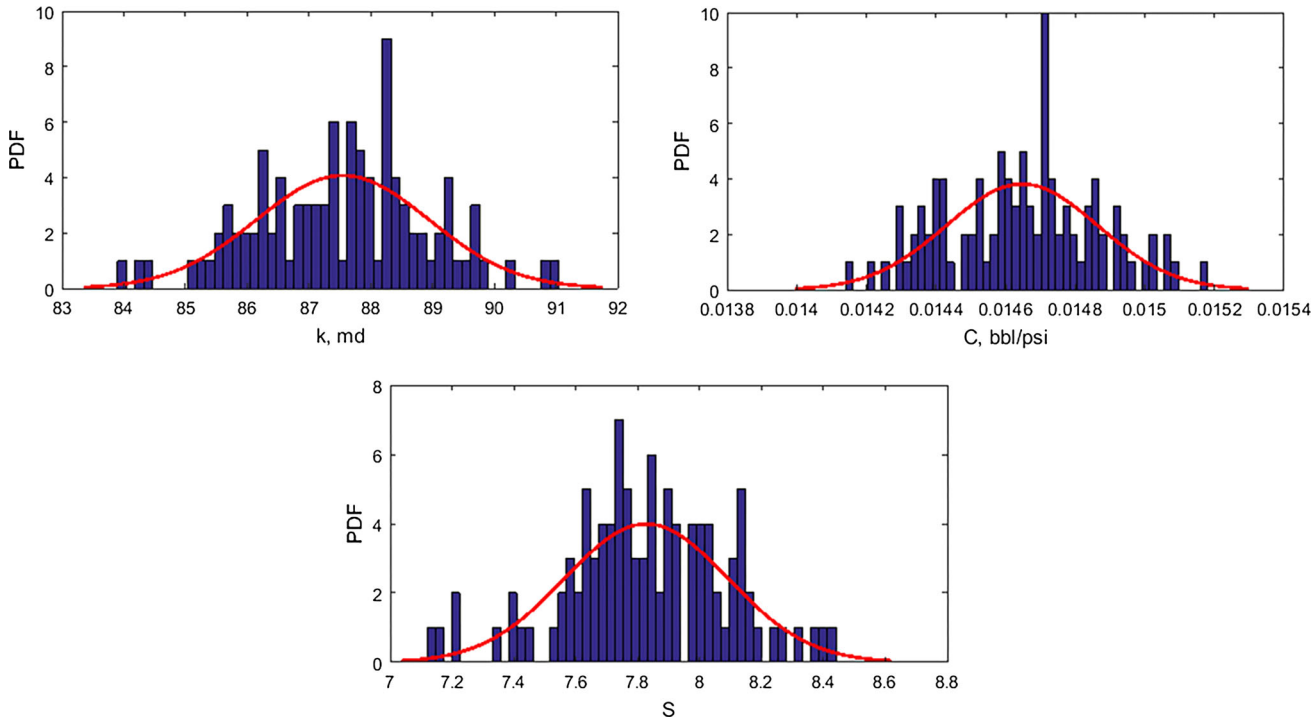

Fig. 3 PDF (probability distribution function) of the reservoir parameters and the corresponding fitted normal curves for the field data belonging to [68]

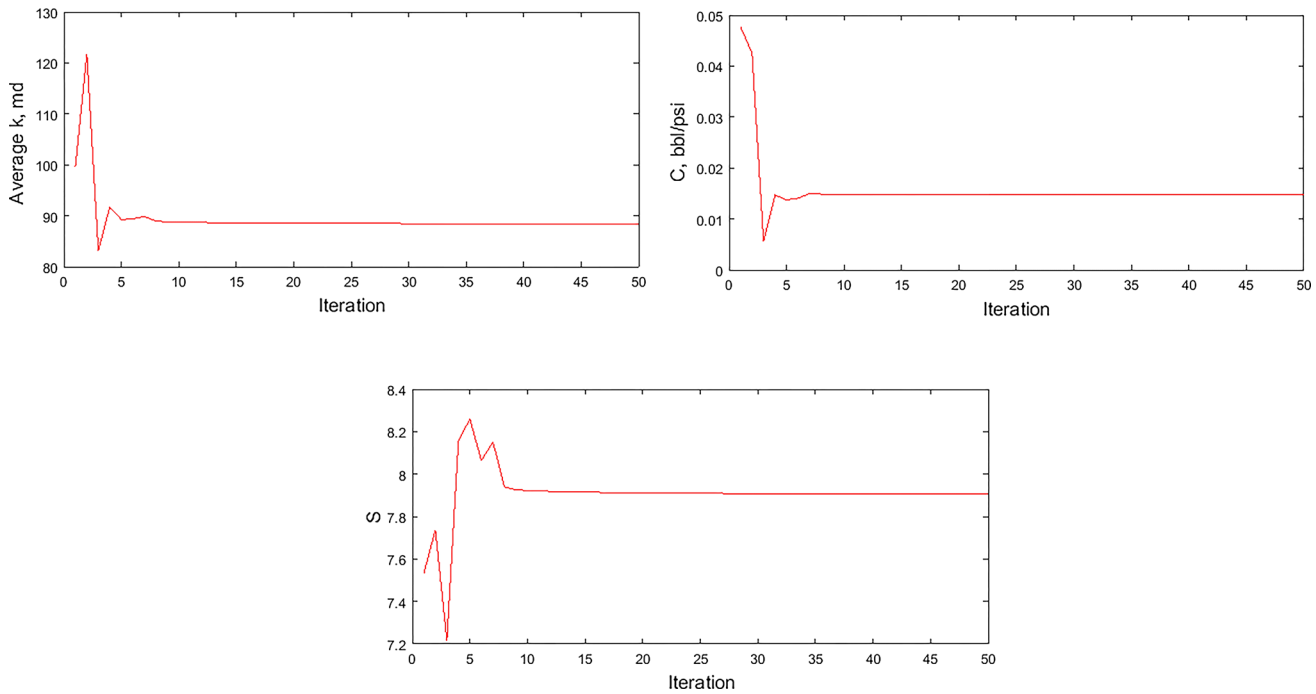

Fig. 4 Average reservoir parameters against iterations for the data taken from [68]

gauge is used as the pressure transducer with gauge resolution of 0.01 *psi* and artificial noise of 0.15 *psi* is added to the data. The distorted derivative data are shown in Fig. 6. The vague at the trough in the derivative data would make it very difficult for any optimization algorithm to work because reservoir models with different fracture storativity ratios, i.e., ω, might mathematically match the data. Also, the distorted data corresponding to the initiation of the last radial flow from the homogenous system would make it tedious for the algorithm to accurately adjust the

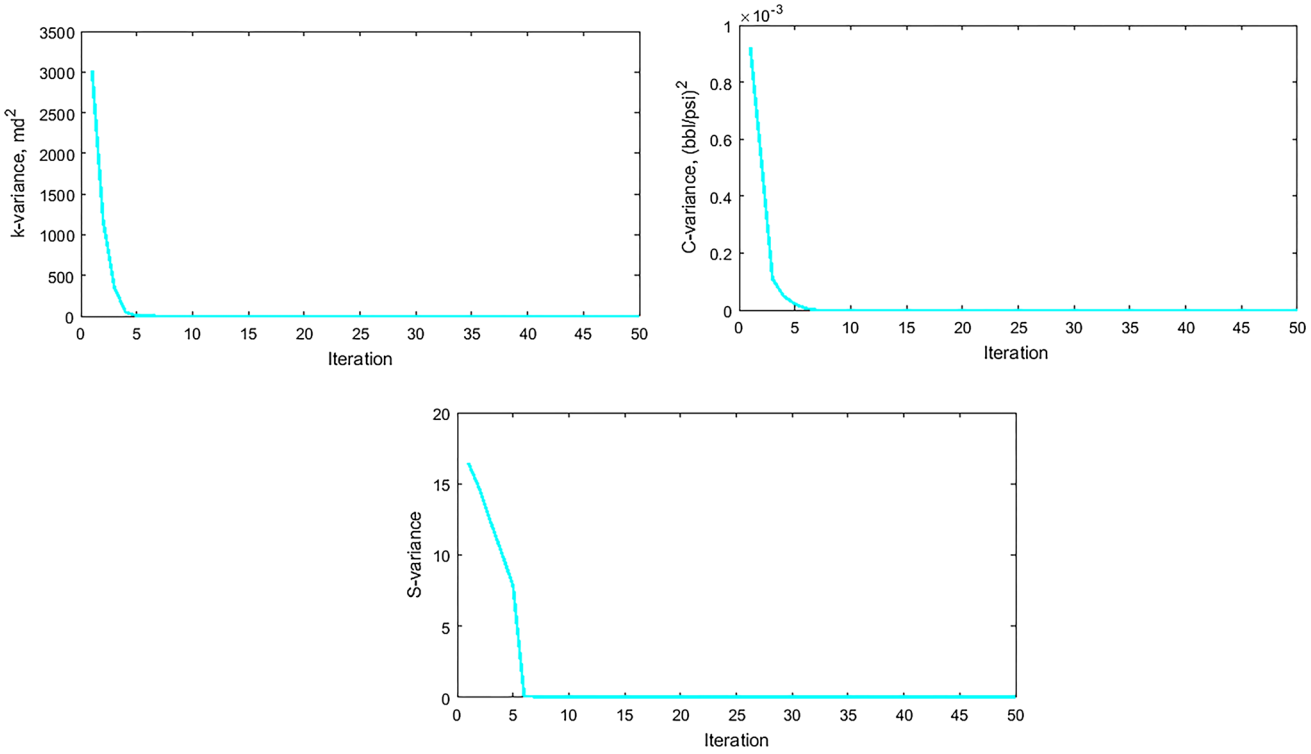

Fig. 5 Variance data for each reservoir variable versus iterations for data belonging to [68]

Table 2 Comparison of the results obtained by the iterative ENKF and the PSO algroithm used by [45] for the homogeneous reservoir model

	k, md	*C*, bbl/*psi*	*S*
Adibifard et al. [45]	87.16	0.0147	7.78
This study	88.4	0.0148	7.91

Table 3 Fluid and rock data for the simulated drawdown test in a fractured dual-porosity system

Φ, fraction	0.1
r_w, ft	0.2
h, ft	50
c_t, psi^{-1}	5×10^{-6}
q, STBD	500
p_i, *psi*	5000
μ, cp	1.0
B_o, Rbbl/STB	1.0
K, md	50
C, bbl/*psi*	0.001
S	− 2
λ	8×10^{-6}
ω	0.1

interporosity flow coefficient with the data. Therefore, through employing the distorted derivative data the robustness of the employed EnKF algorithm over the ambiguous data would be verified.

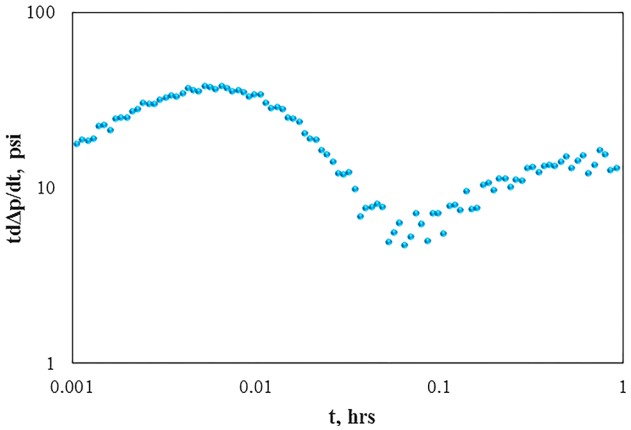

Fig. 6 Logarithmic plot of derivative data versus well-test time for the simulated drawdown test belonging to a dual-porosity system

The amount of the noise included at the pressure-derivative data was proportional to each data point by the $0.05 \times t\mathrm{d}p/\mathrm{d}t$ expression. Again, 200 ensembles were used within the algorithm and calculations were continued for 50 iterations. Different realizations of the observational data are depicted graphically in Fig. 7.

Contrary to the homogenous model, because of the small amounts of the C, λ, and ω and also the increased complexity of the problem due to the higher number of state parameters of the system, the $\log(X)$ of the mentioned

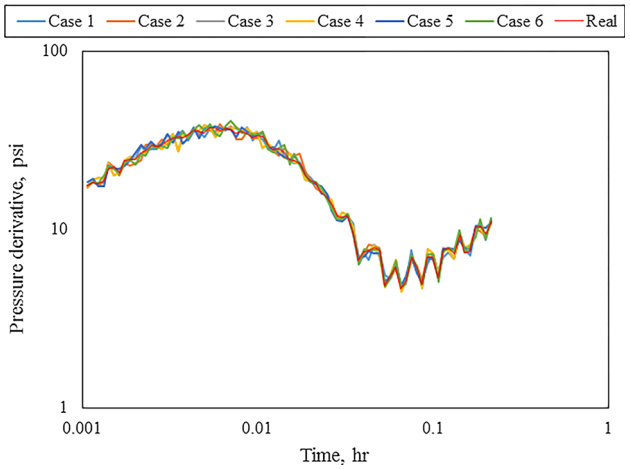

Fig. 7 Different realizations of the measurements by inclusion of the Gaussian noise for the simulated dual-porosity model

parameters was used for the calculations to assure spanning the search space for those small-range parameters. Calculations were made, and the PDF distribution of the corresponding state parameters is illustrated in Fig. 8. Convergence of the mean of the parameters is also shown in Fig. 9. Figures 8 and 9 clearly show that the convergence occurs very fast despite the higher complexity of the system with the increased number of unknown parameters. Most notably, the stabilization of the mean happens before the tenth iteration almost for all of the state parameters which unveils both the speed and robustness of the algorithm.

The estimated reservoir parameters that are the mean parameters at the last iteration are presented in Table 4 along with their corresponding relative error. Accordingly, the best reservoir model using the distorted derivative data is illustrated in Fig. 10. The maximum relative error is below six percent for the estimated parameters, which ultimately proves the robustness of the developed algorithm at this study in dealing with moderately distorted noisy data.

Additionally, the meta-heuristic PSO (particle swarm optimization) algorithm was applied over the tested data and average of the unknown reservoir parameters and their variances are plotted versus the iterations in Fig. 11. The population size and number of iterations for the PSO algorithm remained the same as the iterative EnKF algorithm for comparison purpose. Evolution of the average and variance data over time for the PSO algorithm unveils that this algorithm fails to achieve convergence in the initial iterations contrary to the iterative EnKF algorithm. This indeed reveals the high convergence of the iterative

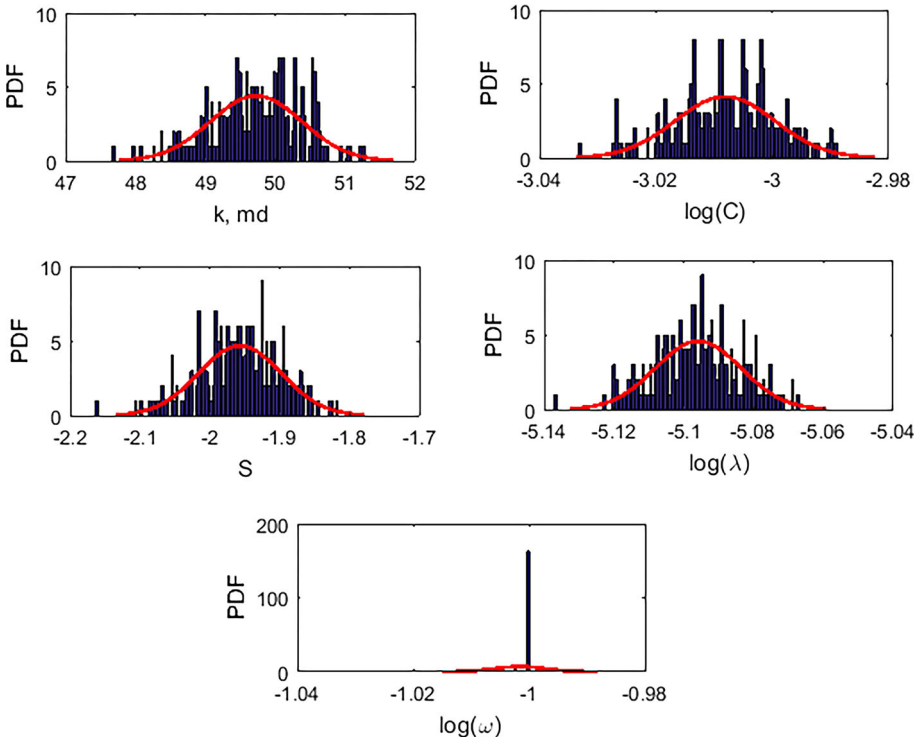

Fig. 8 PDF (probability distribution function) data and the corresponding fitted normal curve for the simulated dual-porosity model

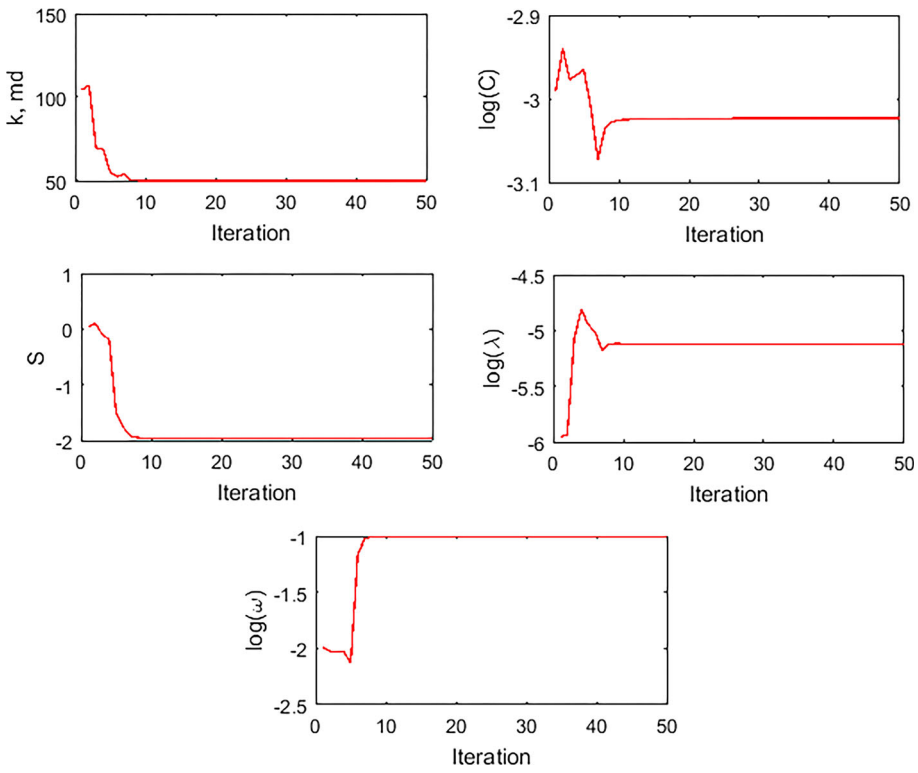

Fig. 9 Mean of the state parameters against iterations for the simulated dual-porosity model

Table 4 Mean of the reservoir parameters obtained through iterative EnKF at the last iteration with corresponding relative error values

Parameter	EnKF estimation	Relative error, %
K, md	49.98	0.04
C, bbl/*psi*	9.48×10^{-4}	5.2
S	-1.97	1.5
λ	7.56×10^{-6}	5.5
ω	0.099	1.0

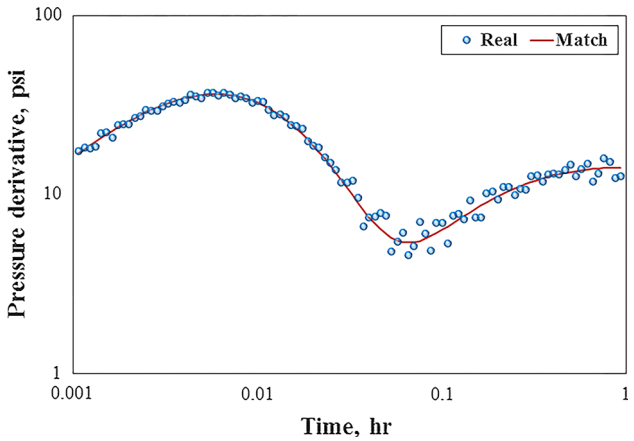

Fig. 10 Obtained graphical match between the best outcome of the iterative EnKF and real noisy data (dual-porosity system)

EnKF algorithm in comparison with one of the well-known meta-heuristic optimization algorithms.

3.3 Homogenous reservoir with a single linear fault

To verify the accuracy of the iterative EnKF model over the faulted reservoirs, another test data are simulated using a commercial well-test software for an infinite acting homogenous reservoir with a single linear fault. To make the data more realistic, an additive noise with an amplitude of 2.5 *psi* is added to the simulated data and also the drift factors of 0.2 *psi*/day were included into the pressure data. Fluid and rock data are given in Table 5, and the distorted pressure-derivative data are plotted in Fig. 12. It clearly shows that the derivative data are distorted in a manner that matching process becomes very difficult, especially for a faulted reservoir model. Hence, this is interesting to study the accuracy of the iterative EnKF for this challenging model. For this model, unknown reservoir parameters include reservoir permeability, wellbore storage coefficient, skin factor, and the perpendicular distance of the fault from the well.

The iterative EnKF method is applied over the derivative data, and the outcomes are provided in Figs. 13, 14 and 15. PDF results at the last iteration are plotted in Fig. 13, and the results approximately show a normal distribution for the unknown reservoir parameters. The mean of the unknown random parameters is provided in Table 6

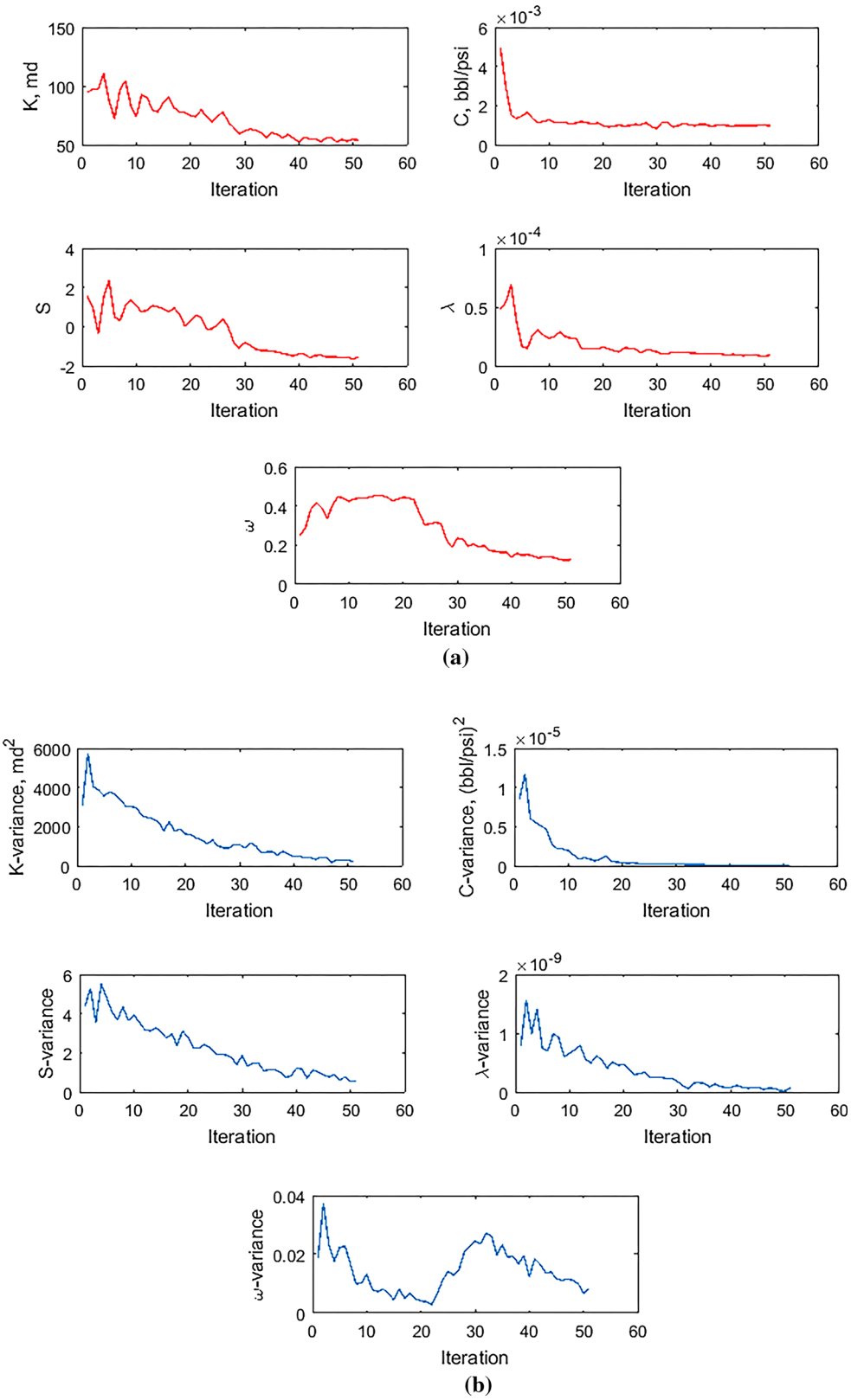

Fig. 11 **a** Evolution of the average of the reservoir parameters and **b** variance of the estimated parameters over time for the simulated dual-porosity model using the PSO (particle swarm optimization) algorithm

Table 5 Fluid and rock data used to generate the pressure data for the homogeneous reservoir with a single fault

Φ, fraction	0.15
r_w, ft	0.25
h, ft	30
c_t, psi^{-1}	5×10^{-6}
q, STBD	800
p_i, psi	5000
μ, cp	1.0
B_o, Rbbl/STB	1.1
K, md	40
C, bbl/psi	0.001
S	+ 2
L_f, ft	200

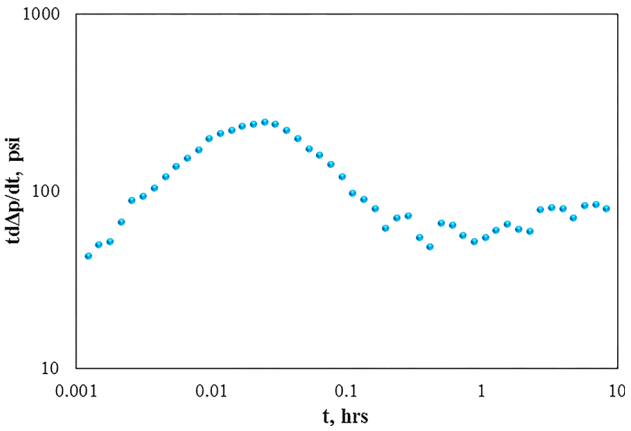

Fig. 12 Generated pressure-derivative data for the homogenous reservoir with a linear fault discontinuity

along with their corresponding relative error, compared to the input values provided to the simulator. From the relative error prospective, the skin factor has the largest estimation error, while the estimation error of the wellbore storage is approximately zero. The second largest estimation error is the estimation of the well distance from the fault, i.e., L_f. The reason behind this might be related to the fact that the skin and L_f are usually highly sensitive to the level of the noise in the observed well-test data.

The convergence and variance plots in Fig. 14 show that the method converges very fast. The variance of the estimated unknown parameters rapidly moves toward zero for all the reservoir parameters. Figure 15 illustrates the estimation of the P10, P50, and P90 for the state parameters of the system for each iteration. Figure 16 demonstrates the high-quality match of the estimated reservoir parameters response to the distorted data and proves the efficiency of the iterative EnKF method to solve the inverse problems for the well-test analysis of the reservoirs with linear discontinuities.

In order to make a comparison between the employed iterative EnKF method and the PSO optimization algorithm, the PSO algorithm is used to estimate the reservoir parameters for this case, and evolution of the average reservoir parameters and their variances are plotted in Fig. 17. As shown in Fig. 17, the variance of the reservoir parameters does not exhibit any stabilization toward the zero horizontal line even after the twentieth iteration. In

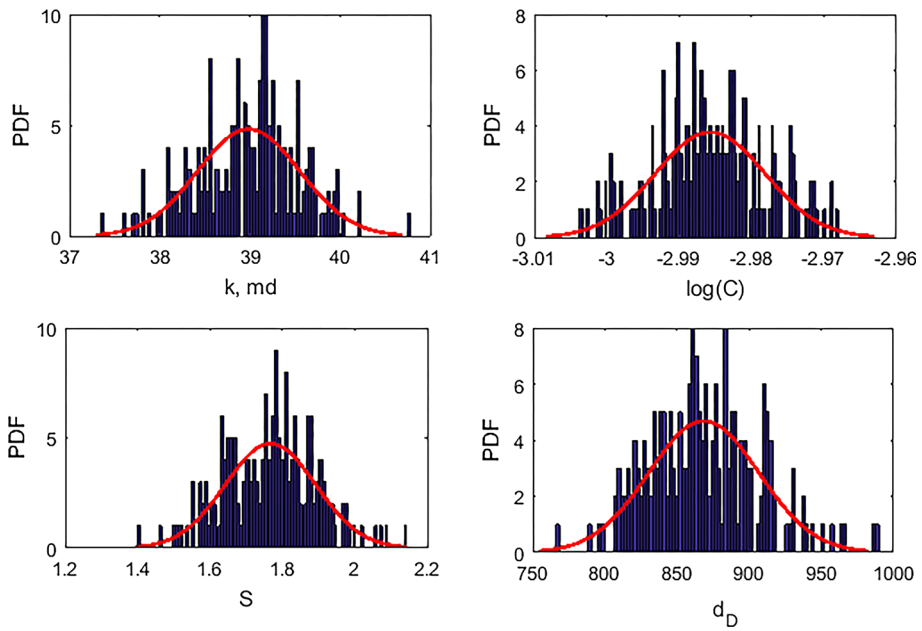

Fig. 13 Obtained PDF for the ensembles at the last iteration with corresponding normal curve for the synthesized homogenous reservoir with a single fault

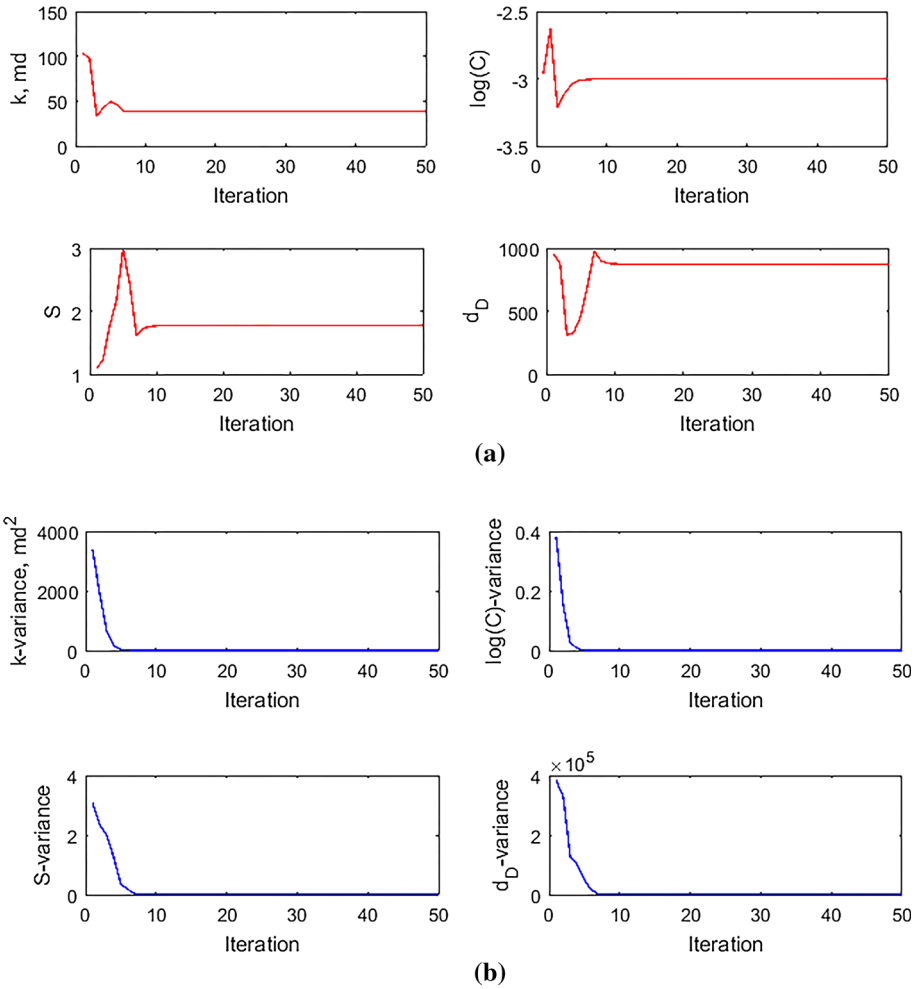

Fig. 14 **a** Average of the reservoir parameters versus iteration and **b** variance of each parameter against the iteration

addition, the average of the reservoir parameters shows some oscillations even after the stabilizations.

4 Conclusion

In this work, we studied the application of the iterative EnKF as a derivative-free type of optimization algorithm for inverse problems arises in the well-test analysis. We used the iterative EnKF method coupled with the Stehfest numerical Laplace inverse algorithm to estimate the unknown reservoir parameters. We conducted three different experiments for a homogenous reservoir model, dual-porosity reservoir model, and a faulted reservoir model to study the accuracy of the proposed algorithm. For all these test cases, the iterative EnKF method gives excellent matches with the true case with a few numbers of iterations. The key findings of this paper are as follows:

- The convergence behavior of the iterative EnKF for three different case studies conducted in this work illustrates a very fast and robust solution to the inverse problems in the well test. The general convergence properties of the iterative EnKF have been previously studied in the literature, both numerically and analytically.
- In high-dimensional cases, that the complexity of the inverse problem increases drastically, the iterative EnKF can give reasonably accurate results with a few numbers of iterations.
- The variances of the state parameters decrease rapidly as the number of iterations increases. This holds for even considerably distorted derivative data, that a large amount of noise is added to the simulated data. In contrast, the well-known PSO (particle swarm optimization) algorithm has very low convergence based on the variance data when it is applied over the simulated tested data.
- The only drawbacks of the iterative EnKF method may be the selection of the tuning parameters, i.e., the variance of the additive noise or the size of ensembles.

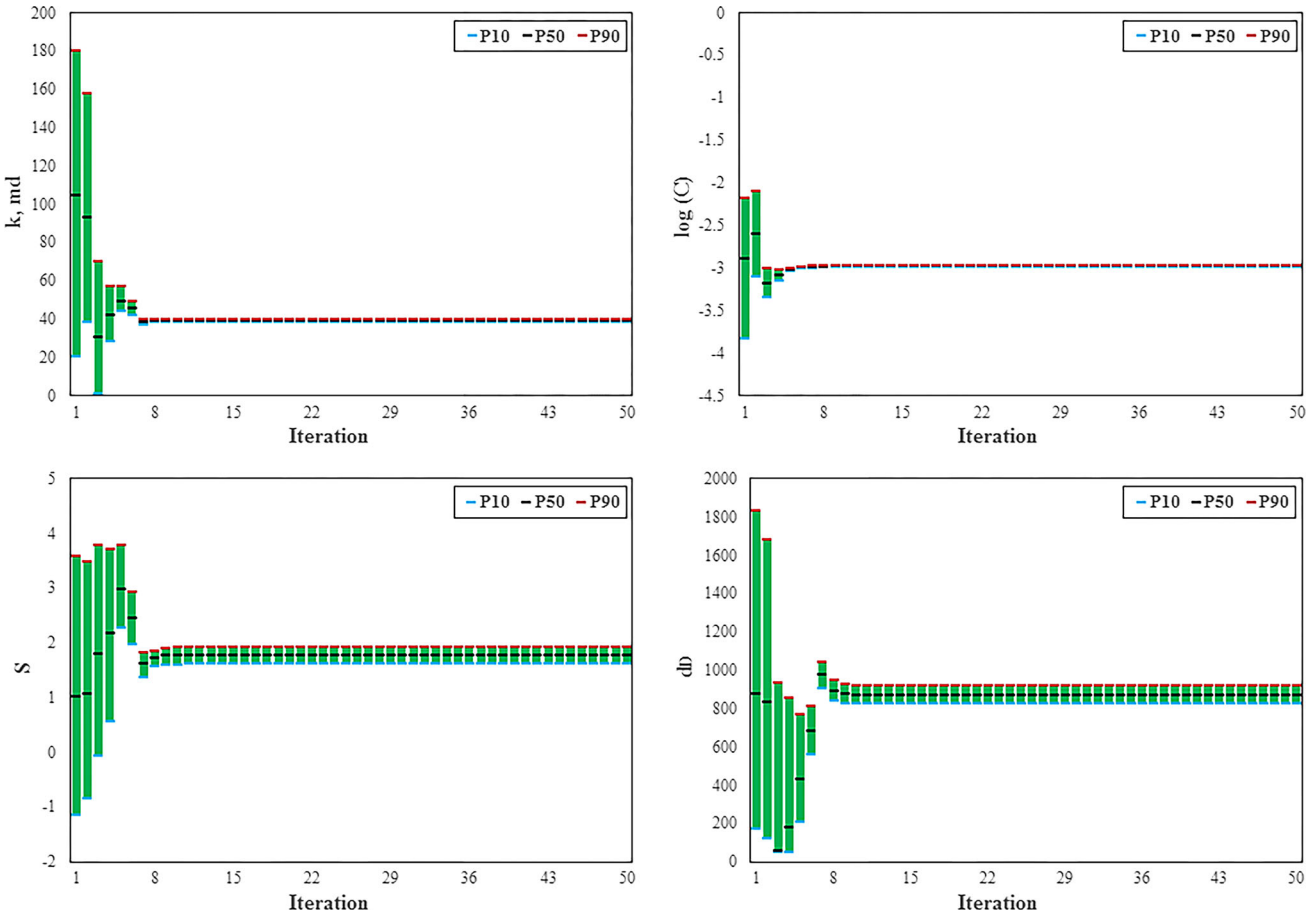

Fig. 15 Evolution of the uncertainty parameters over iterations for the unknown reservoir parameters

Table 6 Estimated reservoir parameters for the homogenous model with a linear fault and corresponding relative error values

Parameter	EnKF estimation	Relative error, %
K, md	39.18	2.05
C, bbl/*psi*	0.001	0
S	1.78	11
L_f, ft	218.23	9.1

This could be the one possible criterion for future research to effectively apply this method to solve the inverse problems in the well-test analysis.

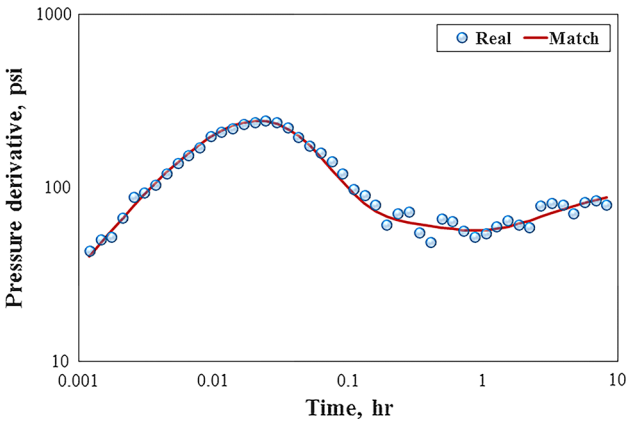

Fig. 16 Final match obtained over the derivative data for the synthesized homogeneous fault model

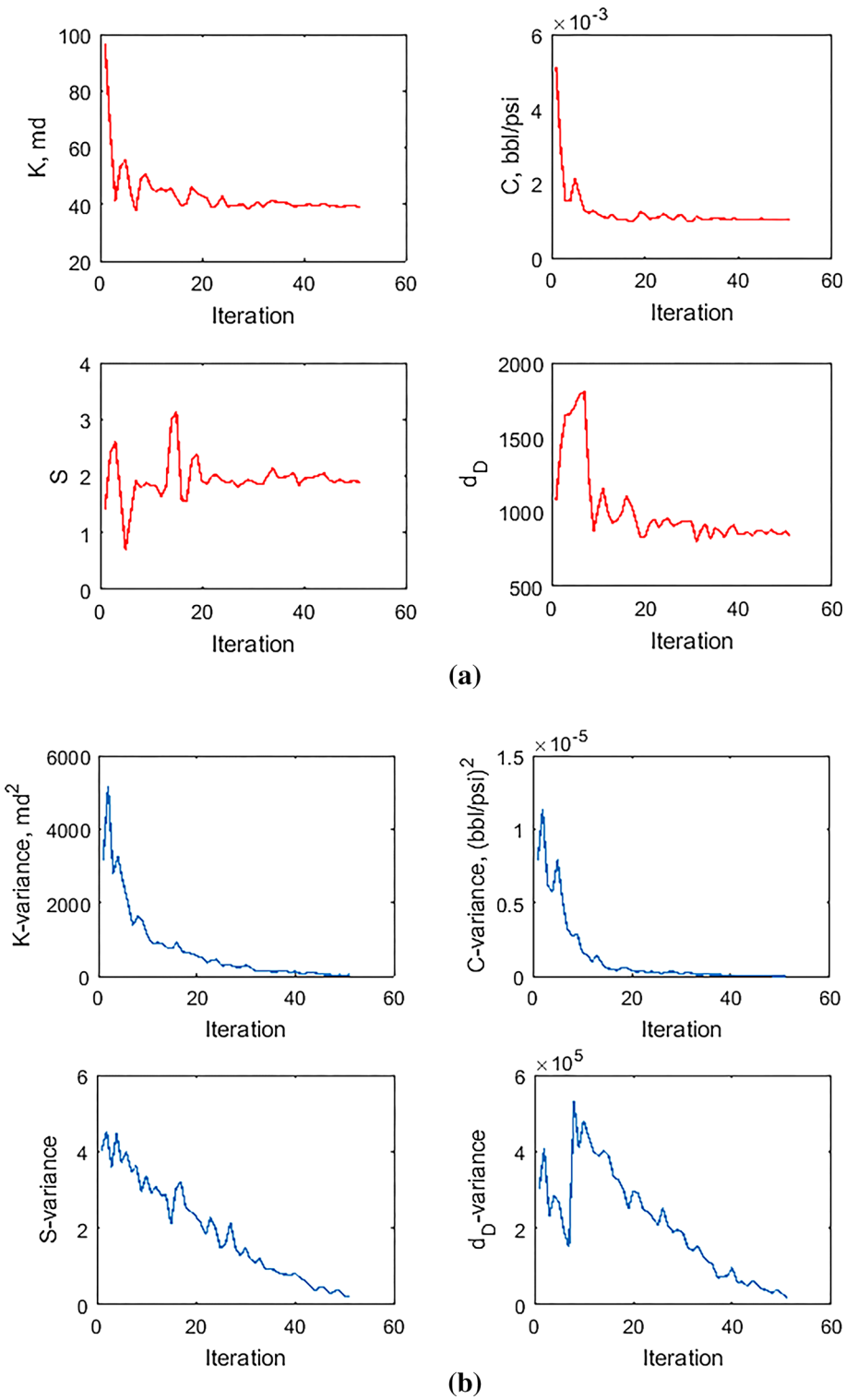

Fig. 17 **a** Evolution of the average of the reservoir parameters and **b** variance of the estimated parameters over time for the simulated linear fault model using the PSO (particle swarm optimization) algorithm

Compliance with ethical standards

Conflict of interest There is no conflict of interest.

Appendix: Well pressure behavior at the Laplace domain

Solution for the well pressure at the Laplace medium is provided at this section for different reservoir systems studied at this paper.

Infinite acting homogenous reservoir [69]

$$\bar{p}_{\mathrm{wD}}(s) = \frac{k_0(\sqrt{s}) + S\sqrt{s}k_1(\sqrt{s})}{s\{\sqrt{s}k_1(\sqrt{s}) + s\mathrm{C}_D[k_0(\sqrt{s}) + S\sqrt{s}k_1(\sqrt{s})]\}}, \tag{15}$$

where S and C_{D} are, respectively, skin factor and the dimensionless wellbore storage coefficient; s is the Laplace parameter; k_0 and k_1 are, respectively, modified Bessel functions of second type with orders zero and one.

Infinite acting dual-porosity reservoir with PSS interporosity flow [70, 71]

$$\bar{p}_{\mathrm{wD}}(s) = \frac{k_0(\sqrt{sf(s)}) + S\sqrt{sf(s)}k_1(\sqrt{sf(s)})}{s\{\sqrt{sf(s)}k_1(\sqrt{sf(s)}) + sC_{\mathrm{D}}[k_0(\sqrt{sf(s)}) + S\sqrt{sf(s)}k_1(\sqrt{sf(s)})]\}}, \tag{16}$$

where $f(s)$ is defined by the following equation:

$$f(s) = \frac{\omega(1-\omega)s + \lambda}{(1-\omega)s + \lambda}, \tag{17}$$

ω is the fracture storativity ratio and λ stands for the interporosity flow coefficient representing how strong is the communication between the matrix and the fracture system. Other parameters are the same as for Eq. 15.

Infinite acting homogenous reservoir with a linear fault [72]

$$\bar{p}_{\mathrm{wD}}(s) = \frac{k_0(\sqrt{s}) + S\sqrt{s}k_1(\sqrt{s}) + k_0(2d_{\mathrm{D}}\sqrt{s})}{s\{\sqrt{s}k_1(\sqrt{s}) + sC_{\mathrm{D}}[k_0(\sqrt{s}) + S\sqrt{s}k_1(\sqrt{s})]\}}, \tag{18}$$

where d_{D} is the fault dimensionless distance defined by $d_{\mathrm{D}} = \frac{L_f}{r_w}$.

References

1. Bazargan H, Christie M, Elsheikh AH, Ahmadi M (2015) Surrogate accelerated sampling of reservoir models with complex structures using sparse polynomial chaos expansion. Adv Water Resour 86:385–399
2. Sambridge M (1999) Geophysical inversion with a neighbourhood algorithm—II. Appraising the ensemble. Geophys J Int 138(3):727–746
3. Poli R, Kennedy J, Blackwell T (2007) Particle swarm optimization. Swarm Intell 1(1):33–57
4. Carter JN, Ballester PJ (2004) A real parameter genetic algorithm for cluster identification in history matching. In: ECMOR IX-9th European conference on the mathematics of oil recovery
5. Li R, Reynolds AC, Oliver DS (2001) History matching of three-phase flow production data. In: SPE reservoir simulation symposium, 2001. Society of Petroleum Engineers
6. Petrovska I, Carter J (2006) Estimation of distribution algorithms for history matching. In: ECMOR X-10th European conference on the mathematics of oil recovery
7. Zhang F, Reynolds AC (2002) Optimization algorithms for automatic history matching of production data. In: ECMOR VIII-8th European conference on the mathematics of oil recovery
8. Oliver DS, Chen Y (2011) Recent progress on reservoir history matching: a review. Comput Geosci 15(1):185–221
9. Wu Z (2000) A Newton-Raphson iterative scheme for integrating multiphase production data into reservoir models. In: SPE/AAPG Western Regional Meeting, 2000. Society of Petroleum Engineers
10. Liu N, Oliver DS (2003) Automatic history matching of geologic facies. In: SPE annual technical conference and exhibition, 2003. Society of Petroleum Engineers
11. Jaynes ET (2003) Probability theory: the logic of science. Cambridge University Press, Cambridge
12. Evensen G (2009) Data assimilation: the ensemble Kalman filter. Springer, New York
13. Aanonsen SI, Nævdal G, Oliver DS, Reynolds AC, Vallès B (2009) The ensemble Kalman filter in reservoir engineering—a review. Spe J 14(03):393–412
14. De Freitas N, Doucet A, Gordon N (2001) An introduction to sequential Monte Carlo methods. SMC Practice Springer, New York
15. Oliver DS, Cunha LB, Reynolds AC (1997) Markov chain Monte Carlo methods for conditioning a permeability field to pressure data. Math Geol 29(1):61–91
16. Ma X, Datta-Gupta A, Efendiev Y (2008) A multistage MCMC method with nonparametric error model for efficient uncertainty quantification in history matching. In: SPE annual technical conference and exhibition, 2008. Society of Petroleum Engineers
17. Rahimi Kh, Adibifard M (2014) Experimental study of the nanoparticles effect on surfactant absorption and oil recovery in one of the iranian oil reservoirs. Petrol Sci Technol 33(1):79–85
18. Sahimi M (2000) Fractal-wavelet neural-network approach to characterization and upscaling of fractured reservoirs. Comput Geosci 26(8):877–905
19. Ali M, Chawathé A (2000) Using artificial intelligence to predict permeability from petrographic data. Comput Geosci 26(8):915–925
20. Al-Anazi A, Gates I (2010) Support vector regression for porosity prediction in a heterogeneous reservoir: a comparative study. Comput Geosci 36(12):1494–1503
21. Al-Bulushi N, King P, Blunt MJ, Kraaijveld M (2012) Artificial neural networks workflow and its application in the petroleum industry. Neural Comput Appl 21(3):409–421
22. Anifowose F, Labadin J, Abdulraheem A (2013) A least-square-driven functional networks type-2 fuzzy logic hybrid model for efficient petroleum reservoir properties prediction. Neural Comput Appl 23(1):179–190
23. Fegh A, Riahi MA, Norouzi GH (2013) Permeability prediction and construction of 3D geological model: application of neural

networks and stochastic approaches in an Iranian gas reservoir. Neural Comput Appl 23(6):1763–1770
24. Fattahi H, Gholami A, Amiribakhtiar MS, Moradi S (2015) Estimation of asphaltene precipitation from titration data: a hybrid support vector regression with harmony search. Neural Comput Appl 26(4):789–798
25. Baziar S, Shahripour HB, Tadayoni M, Nabi-Bidhendi M (2016) Prediction of water saturation in a tight gas sandstone reservoir by using four intelligent methods: a comparative study. Neural Comput Appl 1–15. https://doi.org/10.1007/s00521-016-2729-2
26. Zoveidavianpoor M, Gharibi A (2016) Applications of type-2 fuzzy logic system: handling the uncertainty associated with candidate-well selection for hydraulic fracturing. Neural Comput Appl 27(7):1831–1851
27. Artun E (2017) Characterizing interwell connectivity in water-flooded reservoirs using data-driven and reduced-physics models: a comparative study. Neural Comput Appl 28(7):1729–1743
28. Helmy T, Hossain MI, Adbulraheem A, Rahman S, Hassan MR, Khoukhi A, Elshafei M (2017) Prediction of non-hydrocarbon gas components in separator by using Hybrid Computational Intelligence models. Neural Comput Appl 28(4):635–649
29. Elkatatny S, Mahmoud M, Tariq Z, Abdulraheem A (2017) New insights into the prediction of heterogeneous carbonate reservoir permeability from well logs using artificial intelligence network. Neural Comput and Appl 1–11. https://doi.org/10.1007/s00521-017-2850-x
30. Alimohammadi S, Amin JS, Nikooee E (2017) Estimation of asphaltene precipitation in light, medium and heavy oils: experimental study and neural network modeling. Neural Comput Appl 28(4):679–694
31. Al-Kaabi A, Lee W (1990) An artificial neural network approach to identify the well test interpretation model: applications. In: SPE annual technical conference and exhibition, 1990. Society of Petroleum Engineers
32. Allain O, Houze O (1992) A practical artificial intelligence application in well test interpretation. In: European petroleum computer conference, 1992. Society of Petroleum Engineers
33. Ershaghi I, Li X, Hassibi M, Shikari Y (1993) A robust neural network model for pattern recognition of pressure transient test data. In: SPE annual technical conference and exhibition, 1993. Society of Petroleum Engineers
34. Athichanagorn S, Horne RN (1995) Automatic parameter estimation from well test data using artificial neural network. In: SPE annual technical conference and exhibition, 1995. Society of Petroleum Engineers
35. Kumoluyi A, Daltaban T, Koncar N, Jones AJ, Archer J (1995) Well reservoir model identification using translation and scale invariant higher order networks. Neural Comput Appl 3(3):128–138
36. Alajmi MN, Ertekin T (2007) The development of an artificial neural network as a pressure transient analysis tool for applications in double-porosity reservoirs. In: Asia Pacific oil and gas conference and exhibition, 2007. Society of Petroleum Engineers
37. Kharrat R, Razavi S (2008) Determination of reservoir model from well test data, using an artificial neural network. Scientia Iranica 15(4):487–493
38. Adibifard M, Tabatabaei-Nejad S, Khodapanah E (2014) artificial neural network (ANN) to estimate reservoir parameters in naturally fractured reservoirs using well test data. J Petrol Sci Eng 122:585–594
39. Adibifard M, Sharifi M (2018) Developing a new semi-analytical pressure transient model for limited extent fault systems. J Porous Media 21 **(accepted)**
40. Barua J, Kucuk F, Gomez-Angulo J (1985) Application of computers in the analysis of well tests from fractured reservoirs. In: SPE California regional meeting, 1985. Society of Petroleum Engineers
41. Menekse K, Onur M, Zeybek M (1995) Analysis of well tests from naturally fractured reservoirs by automated type-curve matching. In: Middle East oil show, 1995. Society of Petroleum Engineers
42. Rosa AJ, Horne R (1995) Automated well test analysis using robust (LAV) nonlinear parameter estimation. SPE Adv Technol Ser 3(01):95–102
43. Nanba T, Horne RN (1992) An improved regression algorithm for automated well-test analysis. SPE Form Eval 7(01):61–69
44. Onur M, Kuchuk FJ (1995) Integrated nonlinear regression analysis of multiprobe wireline formation tester packer and probe pressures and flow rate measurements. In: SPE annual technical conference and exhibition, 1999. Society of Petroleum Engineers
45. Adibifard M, Bashiri G, Roayaei E, Emad MA (2016) Using particle swarm optimization (PSO) algorithm in nonlinear regression well test analysis and its comparison with Levenberg–Marquardt algorithm. Int J Appl Metaheuristic Comput (IJAMC) 7(3):1–23
46. Zhou H, Gómez-Hernández JJ, Li L (2014) Inverse methods in hydrogeology: evolution and recent trends. Adv Water Resour 63:22–37
47. Iglesias MA, Law KJ, Stuart AM (2013) Ensemble Kalman methods for inverse problems. Inverse Prob 29(4):045001
48. Keppenne CL, Rienecker MM (2002) Initial testing of a massively parallel ensemble Kalman filter with the Poseidon isopycnal ocean general circulation model. Mon Weather Rev 130(12):2951–2965
49. Bertino L, Evensen G, Wackernagel H (2003) Sequential data assimilation techniques in oceanography. Int Stat Rev 71(2):223–241
50. Zhang S, Harrison M, Wittenberg A, Rosati A, Anderson J, Balaji V (2005) Initialization of an ENSO forecast system using a parallelized ensemble filter. Mon Weather Rev 133(11):3176–3201
51. Houtekamer PL, Mitchell HL (2001) A sequential ensemble Kalman filter for atmospheric data assimilation. Mon Weather Rev 129(1):123–137
52. Szunyogh I, Kostelich EJ, Gyarmati G, Patil D, Hunt BR, Kalnay E, Ott E, Yorke JA (2005) Assessing a local ensemble Kalman filter: perfect model experiments with the National Centers for Environmental Prediction global model. Tellus A 57(4):528–545
53. Reichle RH, McLaughlin DB, Entekhabi D (2002) Hydrologic data assimilation with the ensemble Kalman filter. Mon Weather Rev 130(1):103–114
54. Moradkhani H, Sorooshian S, Gupta HV, Houser PR (2005) Dual state-parameter estimation of hydrological models using ensemble Kalman filter. Adv Water Resour 28(2):135–147
55. Andreadis KM, Lettenmaier DP (2006) Assimilating remotely sensed snow observations into a macroscale hydrology model. Adv Water Resour 29(6):872–886
56. Liu N, Oliver DS (2005) Ensemble Kalman filter for automatic history matching of geologic facies. J Petrol Sci Eng 47(3):147–161
57. Gu Y, Oliver DS (2007) An iterative ensemble Kalman filter for multiphase fluid flow data assimilation. Spe J 12(04):438–446
58. Kalnay E (2003) Atmospheric modeling, data assimilation and predictability. Cambridge University Press, Cambridge
59. Iglesias MA, Law KJ, Stuart AM (2013) Evaluation of Gaussian approximations for data assimilation in reservoir models. Comput Geosci 17(5):851–885
60. Kalman RE (1960) A new approach to linear filtering and prediction problems. J Basic Eng 82(1):35–45

61. Welch G, Bishop G (1995) An introduction to the kalman filter. University of North Carolina, Department of Computer Science. TR 95-041
62. Gillijns S, Mendoza OB, Chandrasekar J, De Moor B, Bernstein D, Ridley A (2006) What is the ensemble Kalman filter and how well does it work? In: American control conference, 2006. IEEE, p 6
63. Evensen G (1994) Sequential data assimilation with a nonlinear quasi-geostrophic model using Monte Carlo methods to forecast error statistics. J Geophys Res: Oceans 99(C5):10143–10162
64. Evensen G (2003) The ensemble Kalman filter: theoretical formulation and practical implementation. Ocean Dyn 53(4):343–367
65. Evensen G. (2002) Sequential data assimilation for nonlinear dynamics: the ensemble kalman filter. In: Pinardi N., Woods J. (eds) Ocean forecasting. Springer, Berlin, Heidelberg
66. Stehfest H (1970) Algorithm 368: numerical inversion of Laplace transforms [D5]. Commun ACM 13(1):47–49
67. Okoye C, Songmuang A, Ghalambor A Application of P'D (1991) In well testing of naturally fractured reservoirs. In: Low permeability reservoirs symposium, 1991. Society of Petroleum Engineers
68. Home RN (1995) Modern well test analysis. Petroway Inc, Palo Alto, p 257p
69. Juniardi I, Ershaghi I (1993) Complexities of using neural network in well test analysis of faulted reservoirs. In: SPE western regional meeting, 1993. Society of Petroleum Engineers
70. Mavor MJ, Cinco-Ley H (1979) Transient pressure behavior of naturally fractured reservoirs. In: SPE California regional meeting, 1979. Society of Petroleum Engineers
71. Da Prat G (1990) Well test analysis for fractured reservoir evaluation, vol 27. Elsevier, Amsterdam
72. Anraku T (1993) Discrimination between reservoir models in well test analysis. Stanford University, Stanford